A web-based Diagnostic Tool for COVID-19 Using Machine Learning on Chest Radiographs (CXR).

E.B. Gueguim Kana[1], M.G. Zebaze Kana[2], A.F. Donfack Kana[3] R.H Azanfack Kenfack*

[1] School of Life Sciences, University of KwaZulu-Natal, South Africa

*Corresponding author kanag@ukzn.ac.za

[2]Natural Science Sector, United Nations Educational, Scientific and Cultural Organization, 7 Place de Fontenoy, 75007 Paris, France

[3]Department of Computer Science, Ahmadu Bello University, Zaria, Nigeria

Abstract

This paper reports the development and web deployment of an inference model for Coronavirus COVID-19 using machine vision on chest radiographs (CXR). The transfer learning from the Residual Network (RESNET-50) was leveraged for model development on CXR images from healthy individuals, bacterial and viral pneumonia, and COVID-19 positives patients. The performance metrics showed an accuracy of 99%, a recall valued of 99.8%, a precision of 99% and an F1 score of 99.8% for COVID-19 inference. The model was further successfully validated on CXR images from an independent repository. The implemented model was deployed with a web graphical user interface for inference (https://medics-inference.onrender.com) for the medical research community; an associated cron job is scheduled to continue the learning process when novel and validated information becomes available.

Introduction

The novel coronavirus outbreak was first identified in December 2019 in Wuha, in Hubei province, China. It is caused by Severe Acute Respiratory Syndrome Coronavirus 2 (SARS-CoV-2)(Stoecklin *et al.,* 2020). The virus has a zoonotic origin and, earlier in 2007 Chen *at al*., pointed out that the presence of a large reservoir of SARS-CoV-like viruses in horseshoe bats, together with the culture of eating exotic mammals in southern China, was a time bomb.

The virus is mainly spread through close contact and via respiratory droplets (cough or sneeze) and through fomites (Centers for Disease Control and Prevention (CDC[a]), 2020). Patients with COVID-19 show clinical manifestations including fever, non-productive cough, dyspnoea, myalgia, fatigue, normal or decreased leukocyte counts, and radiographic evidence of pneumonia (Huang, 2019). The Virus has spike-like S proteins surrounding its envelope structure which mediates its attachment to specific receptors on lung cells called the ACE2 receptors using a "key and lock" tactic, facilitating viral entry into the host cell (Tai, 2019). This leads to an inflammatory process in the lungs, causing shortness of breath and in more severe cases, there is a release of cytokines in the bloodstream, thus damaging vital organs.

An exponential spread of this disease has since been observed globally, and the World Health Organization (WHO) declared it as a Public Health Emergency of International Concern on 30 January 2020, and subsequently recognized COVID-19 as a pandemic on 11 March 2020 (WHO, 2020). In the absence of vaccine, and proven drugs to control the pandemic and prevent the collapse of global care system, WHO has recommended countries to isolate, test, treat and trace.

Radiology observations of COVID-19 infected individuals show bilateral multifocal consolidations (fluid or other products of inflammation filling pulmonary air space) that may progress to involve entire lungs. There is also a presence of small pleural effusions which is an abnormal fluid developed in the spaces around the lungs (Kampalath, 2020). Thus there is presence of glass patterned areas, which affect both lungs even in the initial stages of the infection, in particular the lower lobes, and especially the posterior segments, with a fundamentally peripheral and subpleural distribution (Figure 1).

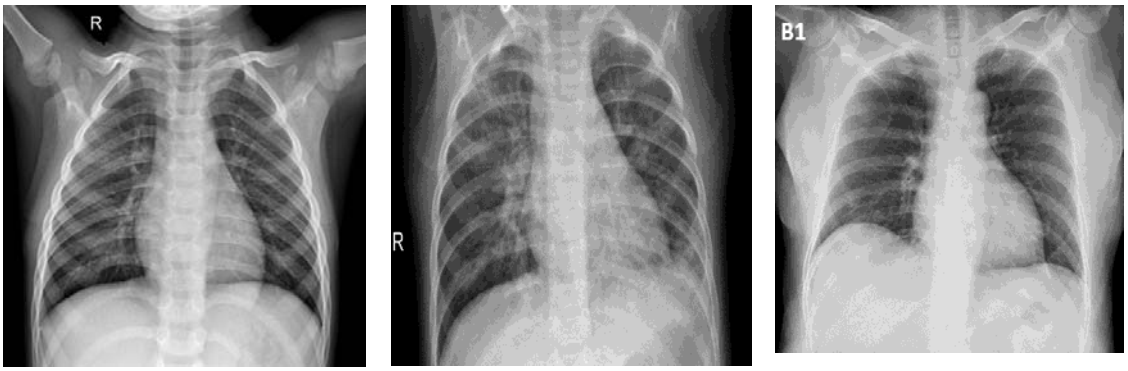

a)Normal CXR b) Viral pneumonia c) COVID-19 positive

Figure 1: CXR images of (a) healthy individual, (b) other Viral or Bacterial pneumonia, (c) COVID-19 positive patient

Currently, to detect and diagnose an infected individual upon clinical suspicion, or monitor the disease, a real-time reverse transcription polymerase chain reaction (rRT-PCR) test is done (CDC[b], 2020) followed by chest radiographs (CXR) and/or computed tomography (CT) scans. rRT-PCR test results may take several hours or days and there is a pronounced shortage of RT-PCR tests kit, unlike the chest CXR which are routinely available with an instant outcome. Italian and British hospitals are beginning to employ CXR as a first-line triage tool due to long reverse transcription polymerase chain reaction (RT-PCR) turnaround times (Wong et al., 2020). There is a growing interest in the use of CXR and CT scans for the screening, diagnosis and management of patients with suspected or known COVID-19 infection. CT scans are more sensitive than RT-PCR, thus a potential advantage of using them (Milagros, 2020). However, the interpretation of CXR and CT-scan is laborious, time-

consuming and requires radiologist expertise. An immediate access to such expertise may not always be available in all clinical settings. These challenges could be addressed with computer vision.

Artificial intelligence image vision in medical diagnosis

There is an increasing interest in the use of Artificial Intelligence (AI) technologies to support disease diagnosis and management in areas of ophthalmology, pathology, cancer detection, radiology or prediction and personalized medicine. The use of Convolutional Deep Neural Network (CDNN) allows for impressive discovery of patterns in medical image datasets, achieving image classification sometimes difficult for human experts (Zhou et al., 2019). The CDNN uses multiple processing layers to learn and represent data with multiple levels of abstraction by applying image analysis filters, or convolutions. The abstracted representation of images within each layer is constructed by convolving multiple filters across the image, producing a feature map that is used as input to the next layer. Thus with this architecture, the image pixels are used as input, then processed to generate the desired classification output. The development and use of Graphical Processing Unit (GPU) instead of CPU and availability of large open-source image datasets for model development have fuelled advances in machine vision (Athanasio et al., 2018).

This study aimed at developing and deploying an inference model for rapid detection of COVID-19 using transfer learning and Machine vision on chest radiographs (CXR).

Materials and Methods

Data source and transformation.

A total of 2507 bacterial or viral pneumonia infected, 2487 healthy individuals and 161 COVID-19 positives CXR images were sourced from two repositories and used for model

development (Kermany *et al.,* 2018; Cohen, 2020). Additional 2585 background class images labelled as "Not Certain" were included. To address the challenge of class imbalance for COVID-19 positive (1:13), data augmentation through contrast transformation (scale: 0.5-1.9) with probability of 0.5 was invoked for this class to achieve a total of 2093. Further data augmentation such as random rotation, horizontal flipping, horizontal and vertical shifting and magnification were not considered for this dataset. Thus a total of 4 classes of healthy individual, bacterial and Viral pneumonia, COVID-19 infected and "Not certain" with 7254 training and 2418 validations image were used. These images were reviewed for their quality, then sized to 350 pixels and normalized according to imagenet statistics.

Model development

The transfer learning of Resnet50 architecture was leveraged for model development. Resnet50 has shown a high performance on benchmark dataset such as Imagenet dataset, a huge database of labelled images containing more than 14 million images which have been hand-annotated and distributed into more than 20,000 classes suitable for training Convolutional Neural Networks. Transfer learning has proven to be a highly effective approach which addresses the limitation in data sizes and lowers the computing cost (Yosinski et al., 2014). It leverages previous knowledge acquired while solving one problem and applying it to a different but related problem (Wang et al., 2020). Thus, through adopting Restnet architecture, the optimized weights gained from previous, and more general trainings were fixed in the lower layers, and only the weights of the upper layers were retrained on chest radiographs (Figure 2).

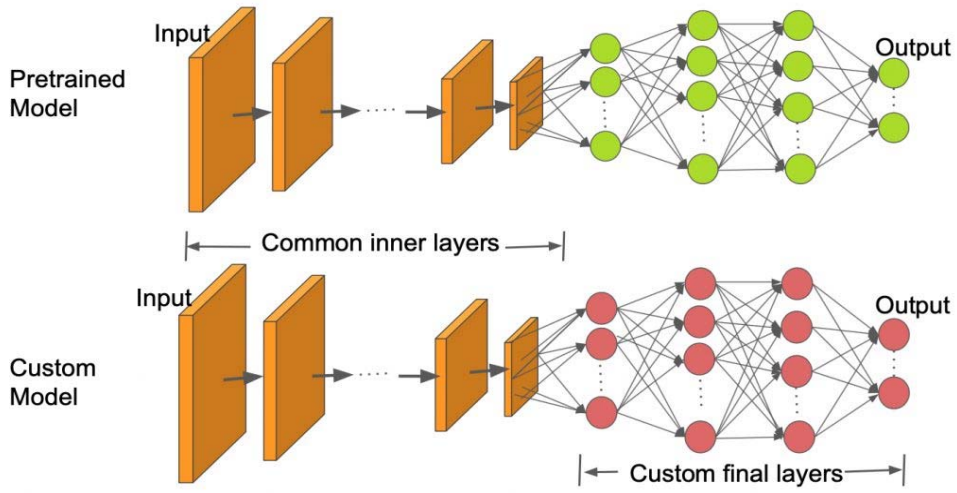

Figure 2: Illustrative diagram of transfer learning using pre-trained model (Nayak, 2019).

The model was developed using python language and trained on the subset of training data with differential learning rate (10^{-4} - 10^{-2}) for 15 epochs on Tesla K80 GPU from google cloud resources. Each epoch corresponded to one complete presentation of the training set to the model.

Model performance metrics

The performance of the model was assessed using the accuracy, precision, recall and F-score. The precision metric is particularly useful when the false positives are of great concern. The recall is important when the impact of false negatives on decision making is high. These were computed using Equations 1 and 2 respectively (Olson, 2008). In some instances, the observed accuracy could be largely contributed by the vast number of true negatives, which may be acceptable for some classes of business decision, whereas false negative and false positive could pose irreversible damage in medical decision, thus F-score was computed using Equation 3.

$$Precision = \frac{tp}{tp + fp} \qquad (1)$$

$$Recall = \frac{tp}{tp + fn} \quad (2)$$

$$F - score = 2 * \frac{Precision * Recall}{Precision + Recall} \quad (3)$$

Model validation on external independent dataset and deployment

The developed model was further validated on a sample data from an additional repository of CXR images (Chowdhury et al., 2020). This repository was curated by expert researchers and medical practitioners consisting of 219 COVID-19 positive images, 1341 normal images and 1345 viral pneumonia images. From this dataset, random samples of 200 images per class were validated on the developed model. The developed model was deployed on the cloud with a web GUI for CXR inference.

Result and Discussion

Model development and performance metrics

The availability of a large labelled dataset of medical images required for the machine vision model development remains a critical challenge due to privacy concerns in data sharing, and the laborious task of data labelling. Transfer learning enables model development using fewer datasets. In this study, Resnet was trained on fewer instances (9672 images) for 30 epochs to obtain an accuracy of 99%. Training was stopped to avoid overfitting as there were no further indications of learning.

The confusion matrix is depicted in Figure 4 based on unseen images for a bacterial or viral pneumonia, out of 2418 instances of images, 2383 were accurately predicted (true positive) and only 35 were wrongly predicted (false positives and false negatives). For COVID-19 class, out of 540 validation instances, 539 were accurately predicted (true positive) and 1 was wrongly predicted as viral or bacterial pneumonia. Zu et al., (2019) reported that in patients with severe disease, their X-ray readings may resemble pneumonia or acute respiratory distress syndrome (ARDS). Notwithstanding, in the case of COVID -19, a single case of a false-

negative outcome for COVID-19 infected individual is a serious concern as it could compromise global efforts to contain the pandemic; similarly, a false positive can cause undue psychological distress, possible contamination if quarantined with infected individuals or unnecessary investigation which places extra burdens on the healthcare system. However, with the current COVID-19 diagnostic procedure, radiography results are used to support the clinical symptomatic examination and could be further confirmed through PCR results. The associated precision and recall values for each class are depicted in table 1.

A false-positive result occurs when an individual is inaccurately assigned to a class, such as a healthy individual categorized as COVID-19 patient and a false negative occurs when an individual who accurately belongs to a given class is excluded from such group.

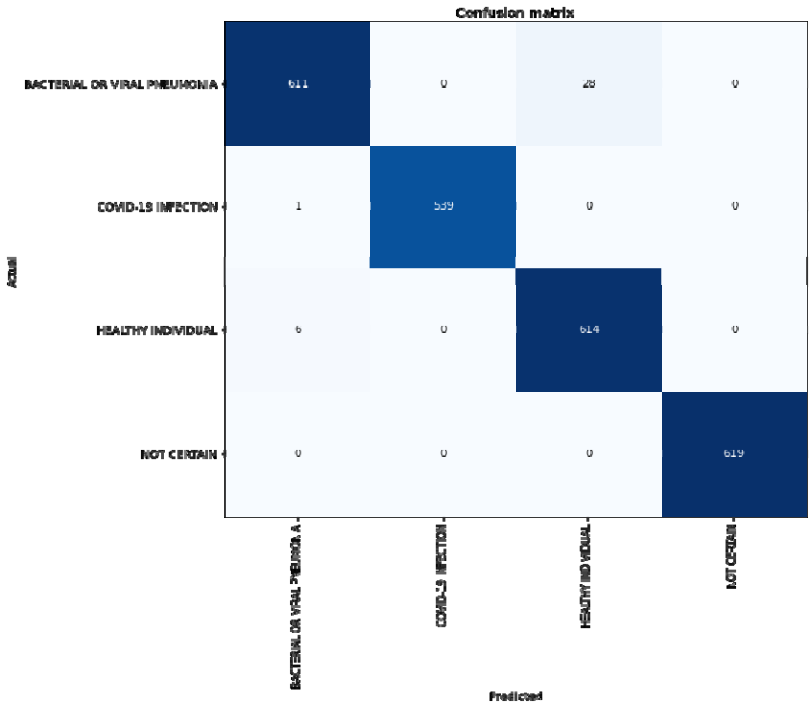

Figure 3: Confusion matrix from validating subset of data.

Table 1: Performance of the classifier

Class	Precision	Recall	Accuracy	F1 measure
bacterial or viral peunomonia	98.8%	97.2%	98.8%	**98%**
COVID-19 Positive	100%	99.8%	100%	**99.8%**
healthy individual	95.6%	99%	95.6%	**97.3%**
Not Certain	100%	100%	100%	**100%**
Average	**99%**	**99%**	**99%**	**99%**

Model performance on an additional independent dataset

When the developed model was assessed on CXR data from an additional repository using a subset of 600 CXR images of COVID-19 positives, viral or bacterial pneumonia and normal persons (200 images per class), accuracies of 97%, 85% and 98% respectively were observed.

Comparison with some existing models

A comparison of the developed model with other reported machine vision models for medical image inference is shown in Table 2 and the corresponding chart for the performance of classifiers is displayed in Figure 4. A noticeable trend in the use of machine vision for medical diagnosis has been observed in the last few years as evidenced in Table 2. The purpose of this comparison was to highlight the similarities in performance metrics and effectiveness of the developed COVID-19 model with other reported machine vision models for medical image inference.

Table 2 Model comparison with some reported AI models on medical images.

MODEL	Model type	Classes	Average accuracy	Precision	Recall	F-Score	References
Computer-Aided Detection and Classification of Abnormalities on Frontal Chest Radiographs	Deep Convolutional Neural Network (GoogLeNet)	Normal Cardiomegal, Pleural effusion, Pulmonary edema, Consolidation, Pneumothorax	82.83%	82.83%	82.83 %	82.83%	Cicero *et al.* (2017)
liver lesion classification with synthetic medical image data augmentation	Deep learning convolutional neural networks	Cyst, Metastasis, Hemangioma	85.7%	92.4%	85.7%	88.92%	Frid-Adar *et al.,* (2018)
brain tumors classification from brain MRIs	Deep learning neural networks	Normal, Glioblastoma, Sarcoma, Metastatic bronchogenic carcinoma	97%	97%	97%	97%	Mohsen *et al.,* (2018)
Detecting tuberculosis (TB) on chest radiographs	Deep convolutional neural networks (AlexNet; GoogLeNet)	pulmonary TB, healthy	98.7%	100%	97.3%	98.63%	Lakhani and Sundaram (2017)
Diagnosis of thyroid nodules using multiple ultrasound images	convolutional neural networks (MXNet)	Malignant thyroid nodules, benign thyroid nodules	87.32%	-	84.22 %	-	Wang *et al.,* (2020).
Diagnosis of thyroid nodules using multiple ultrasound images	Neural network	Malignant thyroid nodules, Benign thyroid nodules	90.31%	95.22%	90.5%	92.8%	Wang *et al*., (2019)
AI System for COVID-19 Diagnosis using chest CT images	Deep convolutional neural net-work	Normal, COVID-19 affected	94.98%	91.53%	94.98%	92.78%	Jin et al., (2020)
diagnosis of COVID-19 infection using chest X-ray	convolutional neural networks with	COVID-19 patient, non COVID-19 patient	99%	81%	78%	79.47%	Castiglioni et al.,(2020)

Inference of COVID-19 on Chest radiographs (CXR). (*This study*)	ResNET50 Recurrent Deep Neural Network with RESNET50	COVID-19, Bacterial and Viral pneumonia, Healthy chest X Ray,	99%	99%	99%	99%	*This study*

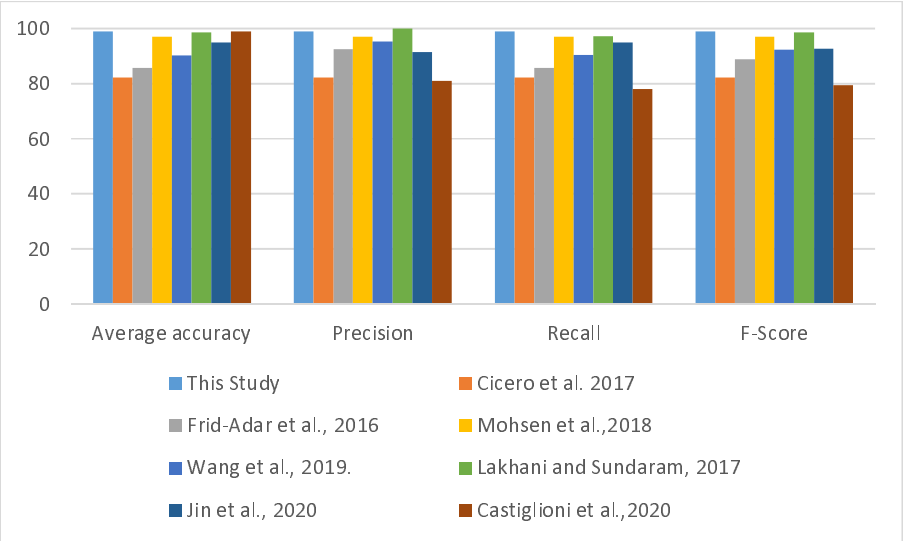

Fig. 4. Comparison chart for the performance of classifiers .

The observed accuracy rate, recall, precision, and F-Measure for all the four classes (COVID-19, Bacterial and Viral pneumonia, Healthy chest X Ray, Not Certain) varied from, 95-100%, 98-100%, 97-100% and 97-100% respectively, and average values of 99% were observed for all the metrics. These performance values compared effectively or slightly better than other reported classifiers in the same terms (Table 2 and Figure 4). Using Deep neural network to diagnose pulmonary tuberculosis, Lakhani and Sundaram (2019) reported performance metrics values of 98.7%, 100%, 97.3% and 98.63% for accuracy, precision, recall and F-score respectively. In the same vein Cicero et al. (2017) investigated the suitability of Deep Convolutional Neural network for detection and classification of abnormalities on frontal chest Radiographs and achieved performance values of 82.83%, 82.83%, 82.83%, 82.83% for accuracy, precision , recall and F-score respectively. In the diagnosis of COVID-19, Jin et al., (2020) used Deep convolutional neural network on chest CT images and obtained 94.98%, 91.53%, 94.98%, 92.78% for accuracy, precision, recall and F-score respectively. Similarly, Castiglioni et al.,(2020) used convolutional neural networks on chest X-ray and obtained 99%, 81%, 78%, 79.47% for accuracy, precision, recall and F-score respectively. These observations

highlight the potential of the developed COVID-19 model to accurately discern the disease pattern on novel CXR images.

Significance of the study for COVID-19 diagnosis

The model's ability to recognise pixels of glass patterned areas on CXR as distinguishing features of COVID-19 and to differentiate these from other viral and pneumonia infected lungs or healthy images resulted from the knowledge gained from the repeated exposures of the neural network to positive training instances, thus providing prediction similar to human experts.

With the rapidly expanding COVID-19 pandemic, the demand for chest radiographs has grown exponentially and proportionally with the number of patients visiting the emergency departments (Milagros, 2020) thus generating a large number of CRX images. Immediate access to expert interpretation may not available or affordable in all clinical settings, thus computer-assisted decision support may be useful to clinicians and radiologists, and for prioritizing cases in a large worklist.

Furthermore, considering that if a massive screening of the population is performed as recommended by the WHO in attempts to curb the infection curve, assuming only 5% the global population (7.8 billion inhabitants) is eventually screened (Worldometer,2020) that would generate 390 million images which need to be reviewed. This will place an unprecedented burden on human experts. Thus automated image analysis tool based on machine learning algorithm, with friendly GUI (Figure 5) will be a key enabler to meet this goal

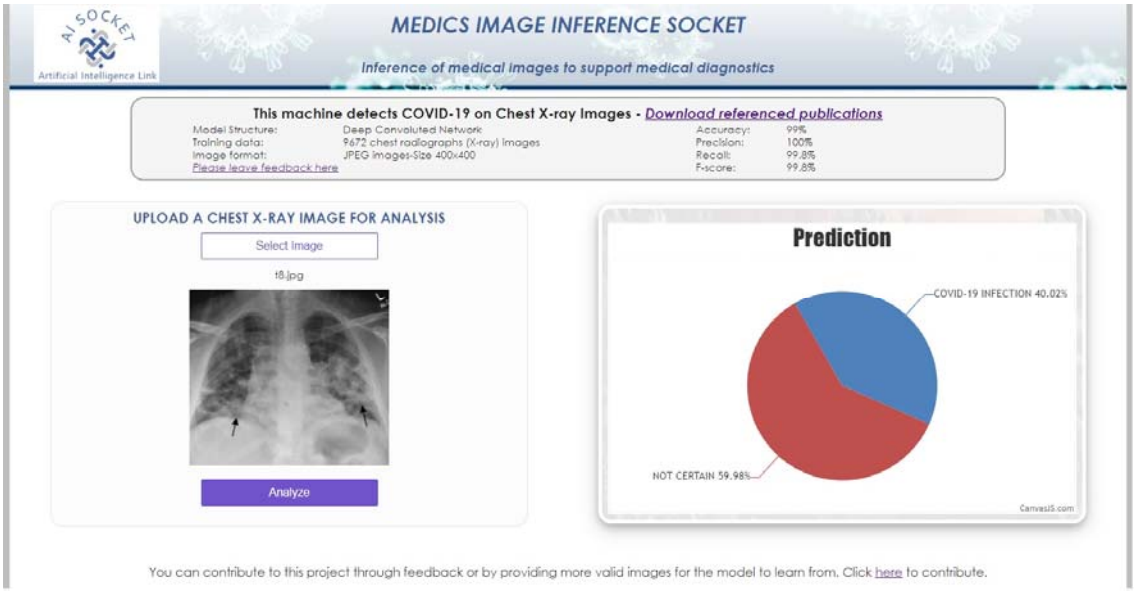

Figure 5: Web graphical User Interface (GUI)

References

Athanasios Voulodimos, Nikolaos Doulamis, Anastasios Doulamis,and Eftychios Protopapadakis, (2018), Deep Learning for Computer Vision: A Brief ReviewComputational Intelligence and Neuroscience https://doi.org/10.1155/2018/7068349.

Castiglioni1 I, Ippolito, D. Interlenghi, M, Monti, C.B., Salvatore, C., Schiaffino, S., Polidori, A., Gandola, D., Messa, C., and Sardanelli, F., (2020) Artificial intelligence applied on chest X-ray can aid in the diagnosis of COVID-19 infection: a first experience from Lombardy, Italy. medRxiv preprint doi: https://doi.org/10.1101/2020.04.08.20040907

Cicero M, Bilbily A, Colak E, et al. (2017), Training and validating a deep convolutional neural network for computer-aided detection and classification of abnormalities on frontal chest radiographs. Invest Radiol. 52:281–287.

Centers for Disease Prevention and Control (CDC[a]) (2020), How COVID-19 Spreads, https://www.cdc.gov/coronavirus/2019-ncov/prevent-getting-sick/how-covid-spreads.html. Retrieved 3 April 2020

Centers for Disease Prevention and Control (CDC[b],) 2020 CDC Diagnostic Test for COVID-19, https://www.cdc.gov/coronavirus/2019-ncov/php/testing.html. retrieved 10 April 2020

C. Jiny, W. Cheny, Y. Caoy, Z. Xu, X. Zhang, L. Deng, C. Zheng, J. Zhou, H. Shi, and J. Feng(2020) Development and Evaluation of an AI System for COVID-19 Diagnosis. medRxiv preprint doi: https://doi.org/10.1101/2020.03.20.20039834

Cohen , 2020, COVID Chest X-ray dataset https://github.com/ieee8023/covid-chestxray-dataset/tree/master/images, retrieved 25 March 2020

C. Huang, Y. Wang, X. Li, et al., (2020), Clinical features of patients infected with 2019novel coronavirus in Wuhan, China, Lancet .https://doi.org/10.1016/S0140-6736(20)30183-5.[16]

H. Mohsen, E.A. El-Dahshan, E.M. El-Horbaty, A.M. Salem, (2018), Classification using Deep Learning Neural Networks for Brain Tumors, *Future Computing and Informatics Journal*, 3(1) 2018.

Kampalath R, 2020, Chest X-ray and CT Scan for COVID-19 viewed 20 April 2020, https://www.verywellhealth.com/medical-imaging-of-covid-19-4801178#citation-1

Kermany, Daniel; Zhang, Kang; Goldbaum, Michael (2018), "Labeled Optical Coherence Tomography (OCT) and Chest X-Ray Images for Classification", Mendeley Data, v2. http://dx.doi.org/10.17632/rscbjbr9sj.2

Lakhani P, Sundaram B. Deep learning at chest radiography: automated classification of pulmonary tuberculosis by using convolutional neural networks. *Radiology*. 2017;284:574–582.

M.E.H. Chowdhury, T. Rahman, A. Khandakar, R. Mazhar, M.A. Kadir, Z.B. Mahbub, K.R. Islam, M.S. Khan, A. Iqbal, N. Al-Emadi, M.B.I. Reaz, "Can AI help in screening Viral and COVID-19 pneumonia?" arXiv preprint, 29 March 2020, https://arxiv.org/abs/2003.13145. https://www.kaggle.com/tawsifurrahman/covid19-radiography-database

M. Frid-Adar, I. Diamant, E. Klang, M. Amitai, J. Goldberger, H. Greenspan GAN-based synthetic medical image augmentation for increased CNN performance in liver lesion classification. *Neurocomputing* 2018 321(10)

Milagros Martí de Gracia, 2020, Imaging the coronavirus disease COVID-19, https://healthcare-in-europe.com/en/news/imaging-the-coronavirus-disease-covid-19.html. Viewed 20 April 2020

Olson, David L.; and Delen, Dursun (2008); *Advanced Data Mining Techniques*, Springer, 1st edition (February 1, 2008), page 138, ISBN 3-540-76916-1

Siu Y, Teoh K, Lo J, Chan C, Kien F, Escriou N, et al. (2008), The M, E, and N structural proteins of the severe acute respiratory syndrome coronavirus are required for efficient assembly, trafficking, and release of virus-like particles. J Virol. 2008;82(22):11318–30.

Stoecklin, S. B., Rolland, P., Silue, Y., Mailles, A., Campese, C., Simondon, A., Mechain, M., Meurice, L., Nguyen, M., Bassi C., Yamani, E., Behillil, S., Ismael,S., Nguyen, D., Malvy, D., Lescure, F. X., Georges, S., Lazarus, C., Tabaï, A., Stempfelet, M., Enouf, V., Coignard, B., Levy-Bruhl, D. and Team, I. First cases of coronavirus disease 2019 (COVID-19) in France: surveillance, investigations and control measures, January 2020. Eurosurveillance, 25(6) :2000094, 2020

Sunita Nayak (2019) Image Classification using Transfer Learning in PyTorch, retrieved 20 March 2020. https://www.learnopencv.com/image-classification-using-transfer-learning-in-pytorch/

Tai, W., He, L., Zhang, X. *et al.* Characterization of the receptor-binding domain (RBD) of 2019 novel coronavirus: implication for development of RBD protein as a viral attachment inhibitor and vaccine. *Cell Mol Immunol* (2020). https://doi.org/10.1038/s41423-020-0400-4

West, Jeremy; Ventura, Dan; Warnick, Sean (2007). "Spring Research Presentation: A Theoretical Foundation for Inductive Transfer". Brigham Young University, College of Physical and Mathematical Sciences. Archived from the original on 2007-08-01. Retrieved 2007-08-05

wong et al Wong HYF, Lam HYS, Fong AH, Leung ST, Chin TW, Lo CSY, Lui MM, Lee JCY, Chiu KW, Chung T, Lee EYP, Wan EYF, Hung FNI, Lam TPW, Kuo M, Ng MY.., 2020. Frequency and

Distribution of Chest Radiographic Findings in COVID-19 Positive Patients.Radiology, Radiology. 2019 Mar 27:201160. doi: 10.1148/radiol.2020201160

"WHO Director-General's opening remarks at the media briefing on COVID-19—11 March 2020". World Health Organization. 11 March 2020. Retrieved 11 March 2020.

Wang, L., Yang, S., Yang, S. *et al.* Automatic thyroid nodule recognition and diagnosis in ultrasound imaging with the YOLOv2 neural network. *World J Surg Onc* **17,** 12 (2019). https://doi.org/10.1186/s12957-019-1558-z

Wang L., Zhang L., Zhu M., Qi X., Yi Z. Automatic Diagnosis for Thyroid Nodules in Ultrasound Images by Deep Neural Networks. Medical Image Analysis, 2010, vol. 61. doi:10.1016/j.media.2020.101665

Wang, L., Yang S., Yang S., Zhao C., Tian G., Gao Y., Chen Y., Lu Y. (2019). Automatic thyroid nodule recognition and diagnosis in ultrasound imaging with the YOLOv2 neural network. World Journal of Surgical Oncology 17(12)

Worldometer, (2020), Current World Population, https://www.worldometers.info/world-population/ retrieved 20 April, 2020

WHO,2020, WHO Director-General's opening remarks at the media briefing on COVID-19 - 11 March 2020. https://www.who.int/dg/speeches/detail/who-director-general-s-opening-remarks-at-the-media-briefing-on-covid-19---11-march-2020. retreive 15 April 2020

Yaqing Wang, Quanming Yao, James T. Kwok, and Lionel M. Ni (2020), Generalizing from a Few Examples: A Survey on Few-Shot Learning, ACM Comput. Surv., Vol. 1, No. 1, https://arxiv.org/pdf/1904.05046.pdf

Yosinski J, Clune J, Bengio Y, and Lipson H. (2014) How transferable are features in deep neural networks? In Advances in Neural Information Processing Systems 27 (NIPS '14), NIPS Foundation, 2014.

Zhou, T, Su Ruan, S., Canu S., (2019) A review: Deep learning for medical image segmentation using multi-modality fusion, Array vol 3-4, September–December 2019, https://doi.org/10.1016/j.array.2019.100004

Zu ZY Jiang MD, Xu PP, et al. Coronavirus Disease 2019 (COVID-19): A Perspective from China. *Radiology*. 2020;200490. doi:10.1148/radiol.2020200490